

Biophysical Journal, Volume 110

Supplemental Information

**Regulating the Membrane Transport Activity and Death of Cells via
Electroosmotic Manipulation**

Tsz Hin Hui, Kin Wah Kwan, Timothy Tak Chun Yip, Hong Wai Fong, Kai Cheong Ngan, Miao Yu, Shuhuai Yao, Alfonso Hin Wan Ngan, and Yuan Lin

A. Fabrication of the electro-osmotic manipulation device

Two identical plastic chambers (with dimension of 4cm x 8cm x 4cm), separated by a partition wall, were fabricated by laser cutting (Universal Laser Systems). A 3.4-cm hole was drilled in the partition wall allowing water and ion exchange between two chambers to take place through a Nafion membrane (Nafion® 117 perfluorinated membrane, Sigma), glued on the wall to cover the hole. The two chambers were then connected with a D.C. power supply (Kikusui Electronics Corp.) so that a voltage difference can be applied across the membrane. Before the test, the device was rinsed by 70% ethanol and washed with 1x Phosphate Buffer Saline five times, followed by 2-hour UV irradiation for sterilization.

B. Intracellular ion concentration measurement

1×10^7 synchronized K562 cells were harvested and preloaded with CoroNa Green (6 μ M, 1h) for Na⁺ and PBFI-AM (6 μ M, 1h) for K⁺ prior to the test (16, 17). The preloaded cells were then subjected to applied voltage (2.0 or -2.0 V) with different durations. Immediately after voltage treatment, two thousand cells, containing PBFI (340-350nm) or CoroNa (488nm), were sequentially excited and their emissions at 425nm (PBFI) or 516nm (CoroNa) were recorded, as shown in Fig. S1. Intracellular concentrations of potassium and sodium were then determined via the method developed in (16) with the so-called dissociation values for each species taken as the same as those used in (16) and (17). The total number of intracellular ions (N_{ion}) can

then be estimated as

$$N_{ion} = M_{ion}V_{cell} \times \text{Avogadro's number} \quad [\text{S1}]$$

where M_{ion} is the measured molar ion concentration and V_{cell} represents the cell volume, calculated from the radii of cells measured by light microscopy.

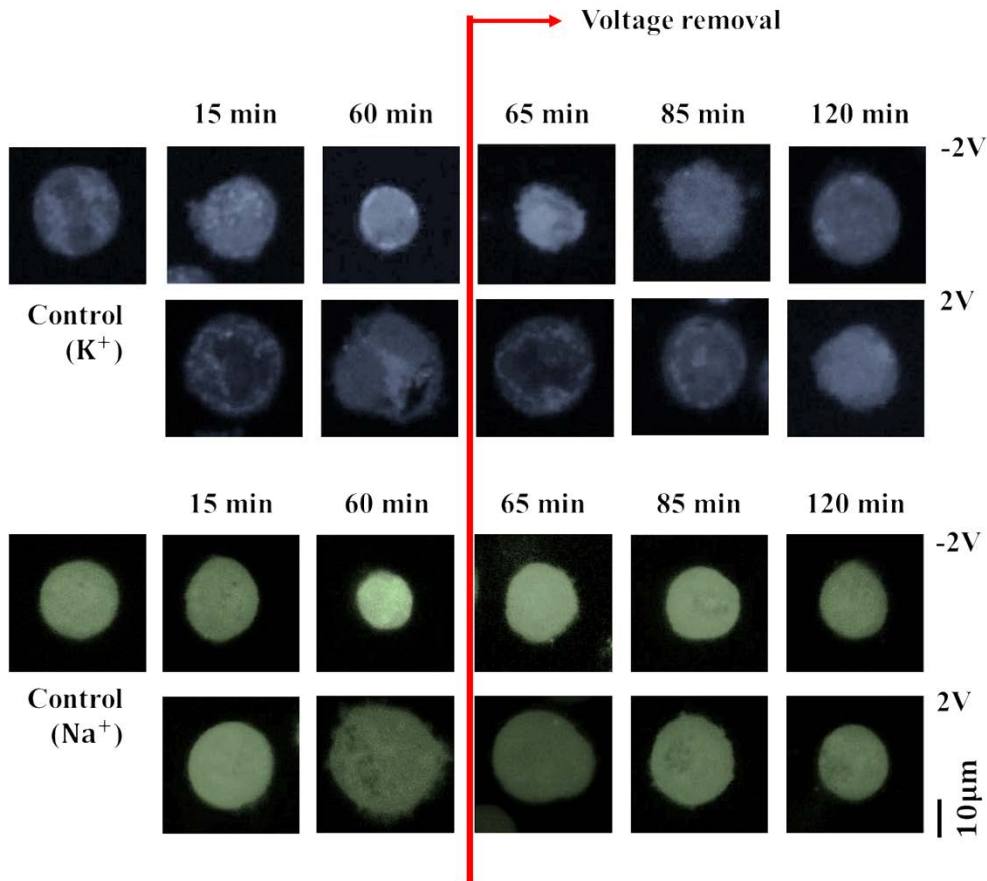


Fig. S1 Fluorescent images of labeled potassium and sodium ions at different time points during voltage treatment. Note that, here cells were maintained in the culture chamber after voltage removal (i.e. Condition B).

Interestingly, as shown in Fig. S2, although the cell size and concentration levels of intracellular K^+ and Na^+ all vary during electro-osmotic manipulation, the total numbers of these two ion species inside the cell remain more or less unchanged.

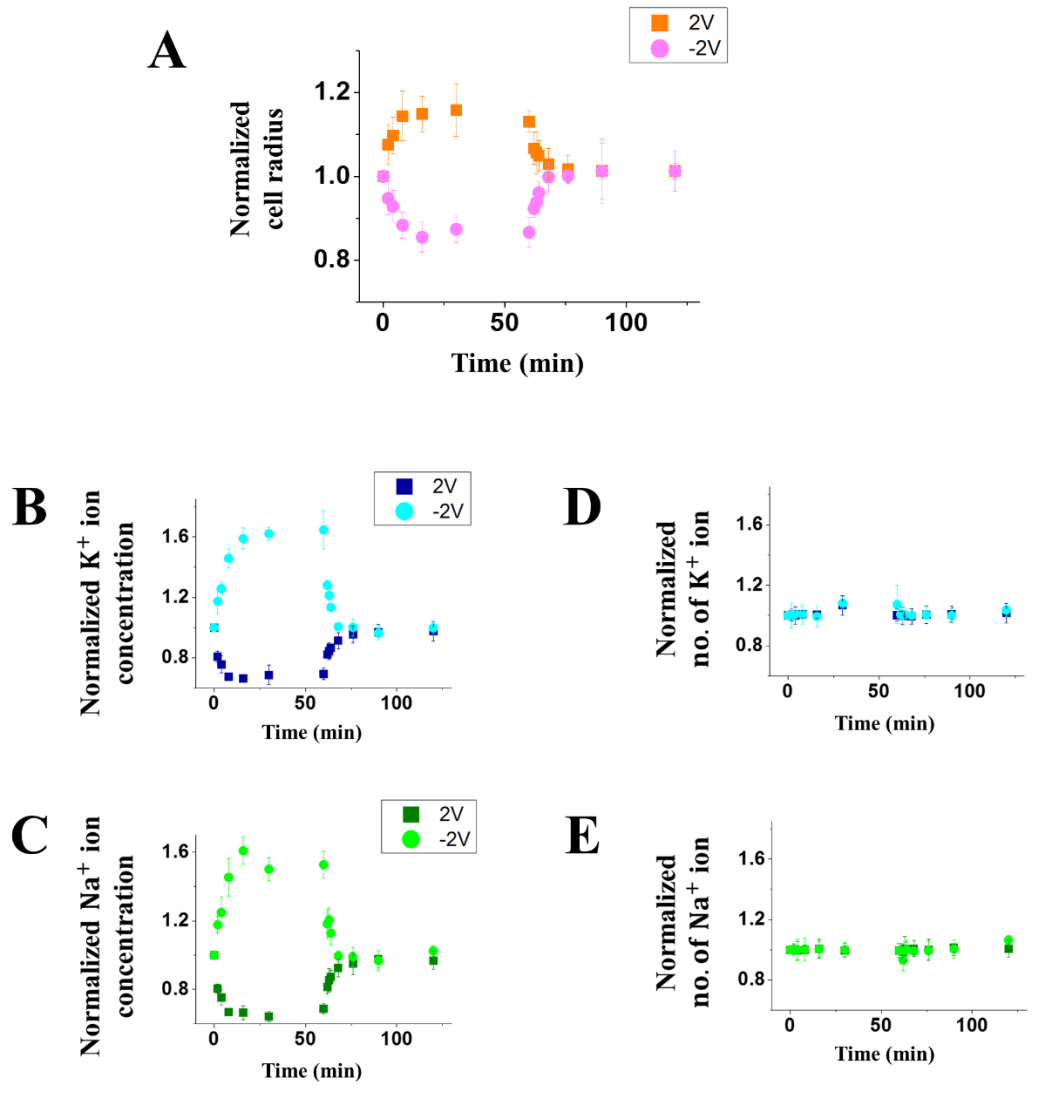


Fig. S2 (A) – Evolution of the radius of K562 cells (normalized by its initial value $r_0 = 10.5 \mu m$) under an applied voltage of 2V or -2V, which was removed after 1 h. (B) – Normalized concentration of K^+ (by its initial value of 317 mM) inside the cell during electro-osmotic manipulation. (C) – Normalized concentration of Na^+ (by

its initial value of 121 mM) inside the cell during electro-osmotic manipulation. (D) –

Total number of intracellular K^+ ion. (E) – Total number of intracellular Na^+ ion.

Cell radii shown in (A) were based on measurements on 30 cells ($p < 0.05$), while a

total of 4000 cells (in two separated trials) were examined by flow cytometry to

render the results given in (B) and (C) with $p < 0.01$.

C. Measuring the cross-membrane potential difference

It is well-known that the phenomenon of ionic shielding will take place around electrodes immersed in electrolytic medium. As such, the potential difference across the Nafion membrane is expected to be different from the applied voltage. To address this issue, the electric potential (with respect to a reference ground value) at different separation distance from the membrane was directly measured by a Reference Electrode (INSESA Instrument) in our experiments. As illustrated in Fig. S3, the potential drop becomes more or less constant at locations more than ~ 0.5 cm away from the membrane. We took this value as the effective cross-membrane potential difference, i.e. Φ_0 , in Eq. [1].

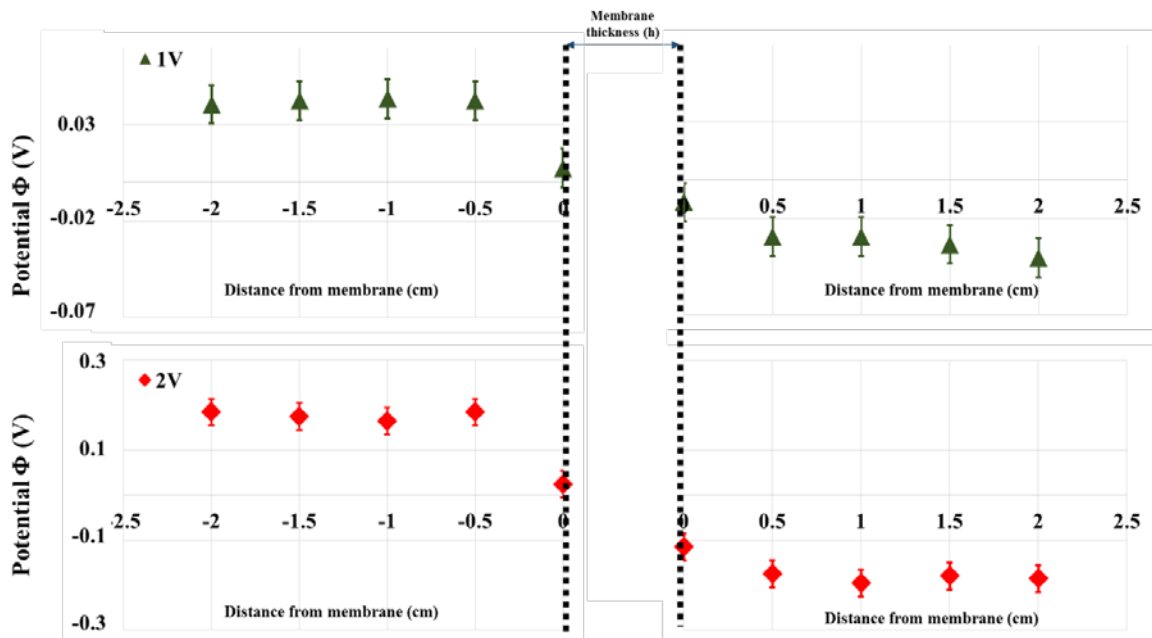


Fig. S3 Measured electric potential as a function of the relative distance from the Nafion membrane.

D. Cell culture. Nasopharyngeal and lung normal-cancer pair cell lines are used in this study. In particular, HONE1 and HK1 were derived from nasopharyngeal carcinoma (NPC) patients and they were paired with the normal immortalized nasopharyngeal epithelial cell lines (NP69 and NP460 with gene transfection by SV40 and telomerase genes respectively). Non-small cell lung carcinoma cell line, A549, was paired up with immortalized normal lung cell line HBE, derived by transfecting bronchial epithelial cells with H-Ras gene. HONE1 and HK1 were cultured in RPMI1640 medium (Gibco) supplemented with 10% fetal bovine serum, FBS (Sigma) and 1% antimycotic antibiotic solution (Sigma). NP69 was cultured in Keratinocyte-SFM medium (Gibco) supplemented with human recombinant Epidermal Growth Factor 1-53 (Gibco) and Bovine Pituitary extract (Gibco). NP460 was cultured in a 1:1 ratio of Defined Keratinocyte-SFM (Gibco) and EpiLife medium (Gibco) supplemented with EpiLife Defined Growth Supplement, i.e. EDGS (Gibco). A549 was in DMEM Glutamax® medium (Gibco) supplemented with 10% FBS (Sigma) and 1% antibiotic solution (Sigma). HBE was cultured in Minimum Essential Medium (MEM), supplemented with 10% FBS.

E. Microfluidic device for cell volume estimation.

Micro-channels (with actual dimensions given in the inset of Fig. 4B) were created following a general PDMS chip fabrication process (S1, S2). Specifically, the master template was developed on a silicon wafer by standard photolithography (SUSS Microtec MA6) and deep reactive ion etching (STS ICP DRIE Silicon Etcher). The resulting chambers for cell loading are 80 μm wide and 15 μm deep while the microchannel is 200 μm long, 10 μm wide, and 5 μm deep. To help releasing the PDMS replica from the master, the silicon wafer was treated with trichloro(1H,1H,2H,2H-perfluorooctyl)silane (Sigma) and put in a vacuum chamber for one hour. Next, PDMS base and curing agent (Sylgard 184, Dow Corning) were mixed with a weight ratio of 10:1, degassed for 30 min, and poured onto the master. After curing the mixture in a 65 °C oven for 4 hours, the PDMS was peeled off from the wafer and cut into small pieces of chips with a blade and holes were punched with a pan needle. The PDMS replica was cleaned by adhesive taper and sonicated in ethanol for 1 min. Finally, the PDMS replica and cover glass (170 μm , Deckglaser) were treated with O₂ plasma for 2 min at 300 mTorr separately and bonded together. To maintain the hydrophilicity, the bonded chip was stored in DI water.

In our experiment, after trypsinization, cells were loaded into the channel where the

cell length (i.e. distance between two poles) is measured optically. 15 cells were measured and a statistical confidence level of no less than 97% by t-test was achieved.

As a control experiment, the size and intracellular content of K562 cells cultured in the chamber of our setup without any voltage applied were also monitored. As shown in Fig. S4, no apparent change in the cellular volume was detected. In addition, the total numbers of intracellular potassium and sodium ions also remain unchanged.

These evidence indicate that cells did not change their state during the manipulation.

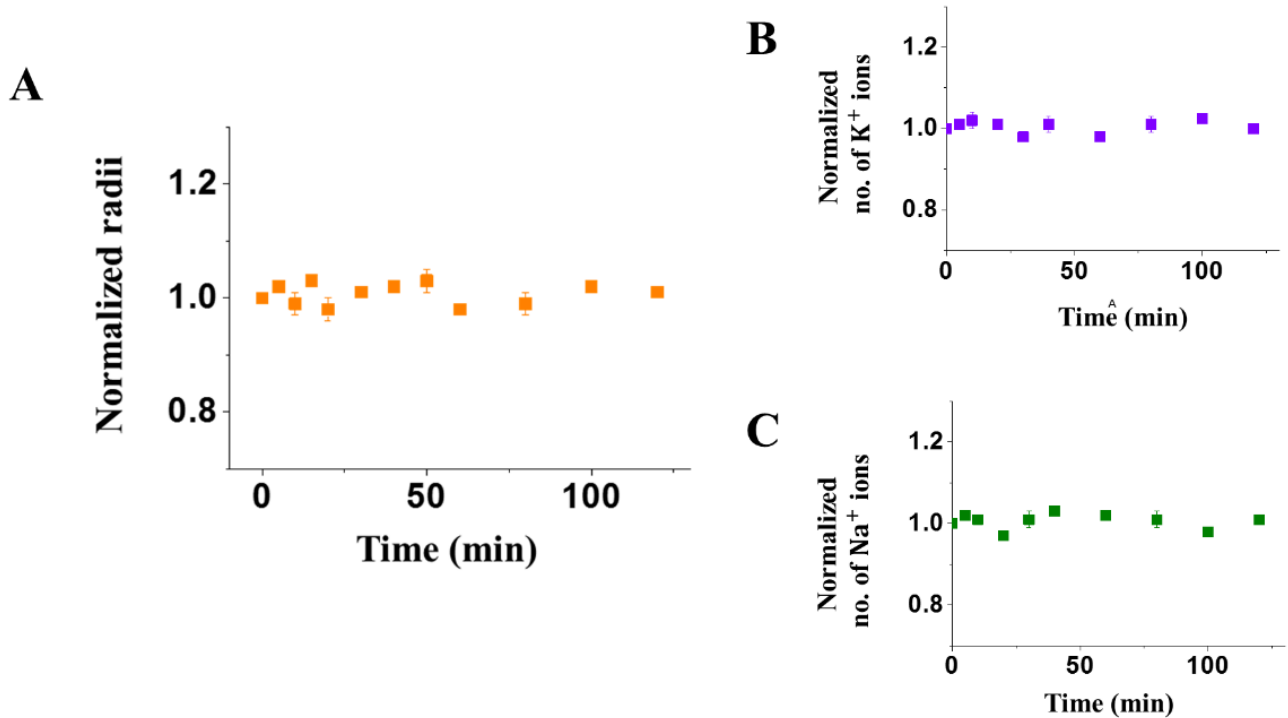


Fig. S4 Measured radii (A) and total number of intracellular K⁺ (B) and Na⁺ (C) of K562 cells cultured in our experiment setup without any applied voltage.

F. Cell viability analysis.

Cells were washed with PBS and stained with Propidium Iodide (PI, Sigma, 10 μ g/mL). Triplicated experiments were performed and 20,000 cells were analyzed by flow cytometry to estimate the death percentage among them.

G. ELISA assays for protein quantification.

The concentrations of AQP1, AQP2 and AQP4 proteins were quantified by the standard ELISA kits (Abnova). Specifically, cell samples were lysed with Cell Extraction Buffer (Novex) and centrifuged to remove solid particulates. 100 μ L of concentration standardized AQPs proteins, including AQP1, AQP2 and AQP4 (Abnova), and lysed cell samples were loaded on each well of the assay plate pre-coated with antibodies that specifically recognize each corresponding AQP protein (Abnova). After that, 100 μ L of Avidin-HRP (Abnova) is added to each microplate well and incubated to yield a protein-conjugated complex as a substrate for labeling. Then, 90 μ L of TMB substrate solution was also added for labelling. The enzyme-substrate reaction was terminated by the addition of 50 μ L sulphuric acid solution and hence the color change. The protein concentration is proportional to the optical density present in the sample, which can be calculated from the calibrated curves obtained by examining standard AQP samples with spectrophotometry at a

wavelength of 450 nm (Fig. S5).

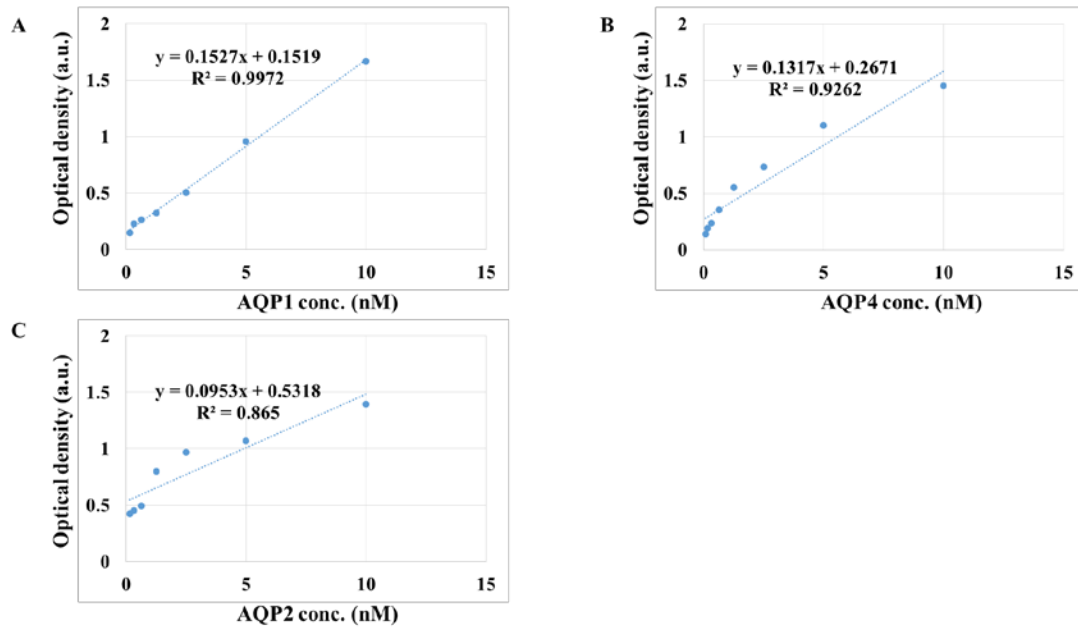


Fig. S5 Calibration curves of AQP proteins from ELISA assays. Protein concentration of the respective AQP proteins were calculated from the calibration function obtained.

H. qPCR for RNA expression determination.

Total RNA was extracted using the RNeasy Micro Kit (Qiagen) and on-column DNase I digestion was performed following the manufacturer's instruction. Next, total RNA was eluted in 14 μ L RNase-free water and the RNA concentration was determined by Qubit® RNA Assay Kit by Qubit® Fluorometer (Life technologies). cDNA was synthesized from 500ng of total RNA in a total volume of 100 μ L using SuperScript III Reverse Transcriptase (Life technologies).

After that, RT-qPCR was carried out using QuantiFast Probe PCR Kit (Qiagen) and an ABI Prism 7000 Sequence Detection System (Applied Biosystems) for the relative quantification of targeted genes. All assays were performed with 1 μ L of cDNA in 25 μ L reactions and the RNA expression of AQP4 was probed by predesigned primer and probe (TaqMan® Gene Expression Assay, Assay ID: Hs00242342_m1). Specifically, the TaqMan Gene Expression Assay was done in triplicate for each sample where 18S rRNA (QuantiFast Probe Assays, QF00530467 Qiagen) served as the endogenous control gene to normalize the data. CT values were obtained by the positive reaction of PCR assay and defined as the number of cycles required for the fluorescent signal to cross the threshold, e.g. the background level. Each replicate CT was normalized by the average CT of 18S rRNA (on a per plate basis), that is by

subtracting the average CT of 18S rRNA from each replicate to give the Δ CT which is equivalent to the log₂ difference between endogenous control and target gene (S3, S4).

Assays were run with ABI Prism 7000 Sequence Detection System (Applied Biosystems) under universal cycling conditions (95°C for 3 min, followed by 40 cycles at 95°C for 10 sec and then 60°C for 30 sec).

I. Western blotting.

Western blot analysis was conducted to determine the expression levels of specific proteins in the sample cell lines, including HONE1, HK1, NP69, NP460, A549, HBE and AQP4-knockdown cells (i.e. HONE1(AQP4D) and A549(AQP4D)). In particular, proteins were harvested at a density of 4×10^7 cells/mL, where all cells were already lysed by ice-cold NP-40 buffer supplemented with phosphatase and protease inhibitors (50 mmol/L sodium vanadate, 0.5 mM phenylmethylsulphonyl fluoride, 2 mg/mL aprotinin, and 0.5 mg/mL leupeptin). The extracted proteins were then separated by sodium dodecyl sulfate polyacrylamide gel electrophoresis (SDS-PAGE), electrotransferred and immobilized on a nitrocellulose membrane. The membrane was blocked with 5% non-fat milk in phosphate-buffered saline containing 0.1% Tween 20 (PBS-T) and incubated at 4 °C with shaking for 12 hours. The membrane was then washed in PBS-T and hybridized with primary antibodies to AQP4 (Sigma) diluted to suitable concentrations in PBS-T for 16 hours. After that, the samples were incubated with their corresponding secondary anti-rabbit antibodies for 30 minutes. The Western blot was stripped by Stripping Buffer (Invitrogen) and re-probed with beta-actin antibody (Invitrogen) to check for equal loading of total proteins.

J. Genetic knockout of AQP4 by siRNA.

Sixty-millimeter plates of confluent A549 cells were treated with 4 nmol/L AQP-4 siRNA (Invitrogen, Sequence: CCGCUGGUCAUGGUCUCCUGGUUGA) for 24 hours where molecules were loaded by Lipofectamine 2000 (Invitrogen) according to the manufacturer's instructions. After that, cells were grown in the culture flasks in OptiMEM serum free medium (Gibco) for another 24 hours where the transfection efficiency can be examined by real-time PCR (refer to Supplementary Materials G). The cell culture was maintained to achieve >90% cell viability. The dead cells were labeled by Trypan blue labeling and counted by hemocytometry.

K. Osmolarity manipulation experiment by microfluidic mixer

To make sure that the appearance of the electric field does not interfere with the functioning of ion channels and hence influence our conclusion, we have conducted an additional experiment where a microfluidic mixer was used to add sucrose to the culture medium. Specifically, the cell culture chamber was connected with a syringe pump (LongerPump) and a microfluidic controller (LongerPump) in this case. Concentrated 1M sucrose solution was prepared by adding 1.71g of sucrose powder (Sigma, Cat#S0389) into 5mL Milli-Q water. The solution was further filtered by 0.22 μ m pore membrane filter (MF-Millipore Membrane Filter) to ensure sterile condition. The solution was then loaded in the syringe and pumped at a perfusion rate of 10.3 μ L/min, 20.5 μ L/min or 41.0 μ L/min into the culture chamber, i.e. a 2mL confocal dish (Nunc). As such, the effective increase in the medium osmolarity, C_{increase} , at the end of perfusion can be calculated as

$$C_{\text{increase}} = C_0 \times \frac{P_f t_f}{V_0 + P_f t_f} \quad [\text{S2}]$$

where C_0 is the initial concentration of sucrose (1M), P_f is the perfusion rate, t_f is the perfusion time and V_0 is the initial volume of the medium inside the chamber (2

mL). Given that the sucrose solution was pumped into the culture chamber for 30 minutes, the total increase in the extracellular osmolarity is estimated to be 133.8 mM, 235.2 mM and 380.8 mM (corresponding to a perfusion rate of 10.3 $\mu\text{L}/\text{min}$, 20.5 $\mu\text{L}/\text{min}$ and 41.0 $\mu\text{L}/\text{min}$) respectively. Interestingly, similar decrease in the volume of K562 cells (compared to that shown in Fig. 2) was observed, refer to Fig. S6B-C. Furthermore, despite some fluctuations, no apparent change in the total number of intracellular Na^+ and K^+ was detected during this process (Fig. S6E and S6G), further confirming the notion that no cross-membrane ion exchange will be triggered by a gradually varied extracellular osmolarity.

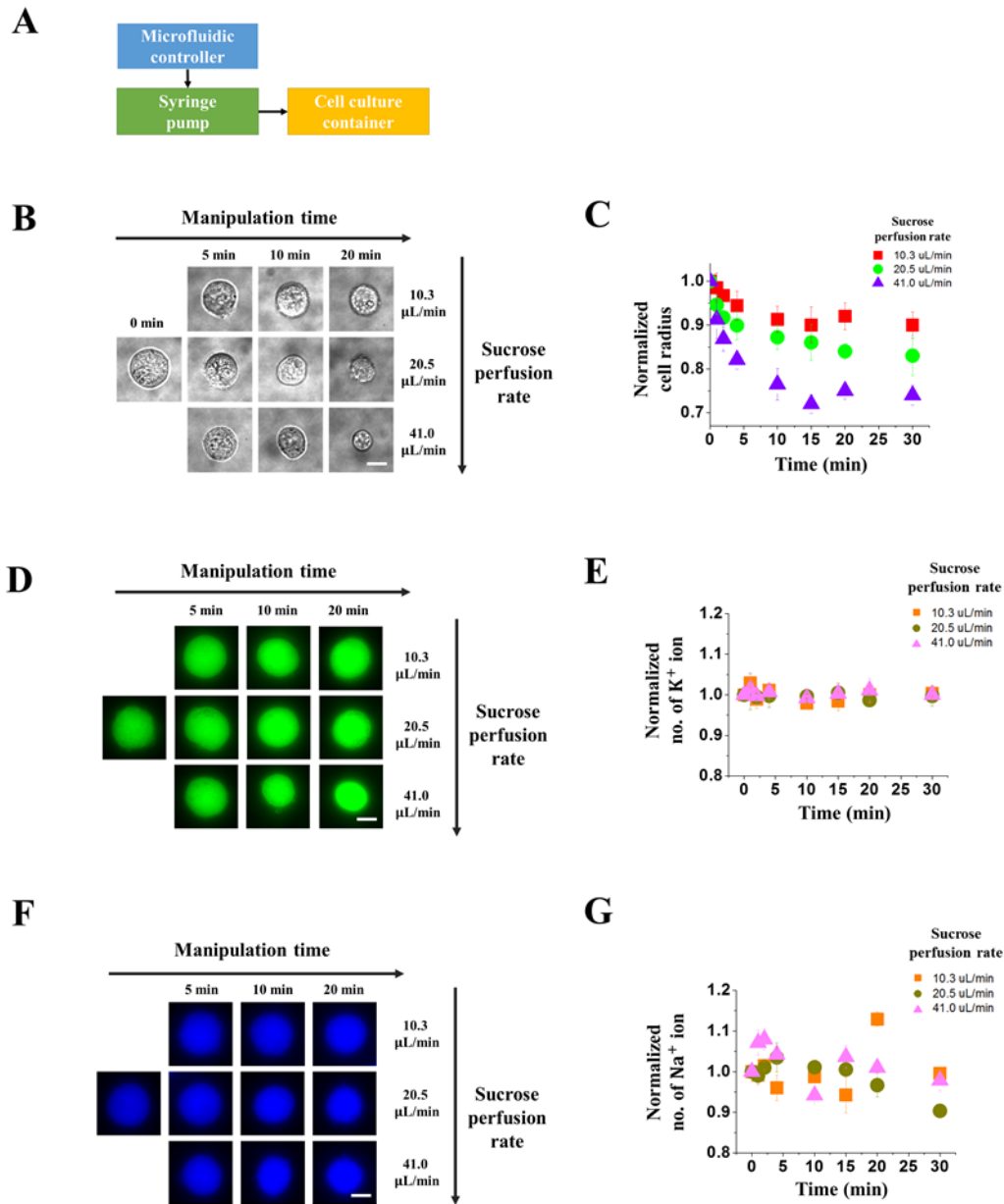


Fig. S6 (A) – Flow chart of using a microfluidic mixer to regulate the cell volume. (B) – Representative micrographs showing the size change of K562 cells under different sucrose perfusion rates. (C) – Change of the mean radius of K562 cells, normalized by its initial value $r_0 = 10.5 \mu\text{m}$. (D) – Fluorescent images of labeled intracellular potassium ions at different time points. (E) – Total number of intracellular K^+ , normalized by its initial value. (F) – Fluorescent images of labeled

intracellular sodium ions at different time points. (G) – Total number of intracellular Na^+ , normalized by its initial value. Cell radii shown in (C) was based on measurements on 30 cells ($p < 0.05$), while a total of 4000 cells (in two separated trials) were examined by flow cytometry to render the results given in (E) and (G) with $p < 0.01$.

Table S1: List of parameters adopted

Parameters	Sym	Adopted values	Reference values		Source
Initial intracellular ion concentration	c_{in}^0	600 mM	600 mM		(9, S5, S6)
Initial concentration of all ions in the left and right compartment	c_0^L, c_0^R	880 mM			Fitting to exp. data
Initial cation concentration in the left and right compartment	c_0^{L+}, c_0^{R+}	380 mM	Na ⁺	K ⁺	Fitting to exp. data
			143.4 mM	84.6 mM	
Initial cell radius of K562 cells	r_0	10.5 μm			Directly measured
Water permeability of cell membrane	L_w	$8 \times 10^{-14} \text{ Pa}^{-1} \text{ s}^{-1} \text{ m}$	in the order of $10^{-14} \text{ Pa}^{-1} \text{ s}^{-1} \text{ m}$		(S7)
Stretching rigidity	K	39 pN/ μm	39 pN/ μm		(S8)
Initial overall cortical tension	γ_0	182 pN/ μm	182 pN/ μm		(9)
Actomyosin tension	γ_A	57.2 pN/ μm	31.5% of the overall cortical tension		(S8)
Electric conductance of Nafion membrane	G	$16 \Omega^{-1} \text{ m}^{-1}$	$8-16 \Omega^{-1} \text{ m}^{-1}$		(15)
Electro-osmotic permeability*	β	$\frac{5 \times 10^{-6}}{\bar{c}} \text{ m}^3/\text{C}$	$\frac{5 \times 10^{-6}}{\bar{c}} \text{ m}^3/\text{C}$		(S9)
Area of the Nafion membrane	A_m	$900 \times 10^{-6} \text{ m}^2$			Experimental condition
Water permeability of Nafion membrane	L_p	$1.6 \times 10^{-13} \frac{\text{m}^2}{\text{Pa} \cdot \text{s}}$	$1.6 \times 10^{-13} \frac{\text{m}^2}{\text{Pa} \cdot \text{s}}$		(20)
Initial volume of left and right	V_0^L, V_0^R	64 cm^3	64 cm^3		Experimental conditions

compartment				
Horizontal cross-section area of two chambers	A_c	16 cm ²	16 cm ²	Experimental condition
Thickness of the Nafion membrane	h	0.1 mm	0.1 mm	Experimental condition

* Electro-osmotic permeability is dependent on \bar{c} , the mean concentration of cations.

References

- S1. Balzer, E. M., Z. Tong, C. D. Paul, W. C. Hung, K. M. Stroka, A. E. Boggs, S. S. Martin, and K. Konstantopoulos. 2012. Physical confinement alters tumor cell adhesion and migration phenotypes. *Faseb j* 26:4045-4056.
- S2. Yu, M., Y. Hou, H. Zhou, and S. Yao. 2015. An on-demand nanofluidic concentrator. *Lab Chip* 15:1524-1532.
- S3. Benjamini, Y., and Y. Hochberg. 1995. Controlling the False Discovery Rate: A Practical and Powerful Approach to Multiple Testing. *Journal of the Royal Statistical Society. Series B (Methodological)* 57:289-300.
- S4. Canales, R. D., Y. Luo, J. C. Willey, B. Austermiller, C. C. Barbacioru, C. Boysen, K. Hunkapiller, R. V. Jensen, C. R. Knight, K. Y. Lee, Y. Ma, B. Maqsodi, A. Papallo, E. H. Peters, K. Poulter, P. L. Ruppel, R. R. Samaha, L. Shi, W. Yang, L. Zhang, and F. M. Goodsaid. 2006. Evaluation of DNA microarray results with quantitative gene expression platforms. *Nat Biotechnol* 24:1115-1122.
- S5. Cividall, G., and D. G. Nathan. 1974. SODIUM AND POTASSIUM CONCENTRATION AND TRANSMEMBRANE FLUXES IN LEUKOCYTES. *Blood* 43:861-869.
- S6. Cameron, I. L., N. K. R. Smith, T. B. Pool, and R. L. Sparks. 1980. INTRACELLULAR CONCENTRATION OF SODIUM AND OTHER ELEMENTS AS RELATED TO MITOGENESIS AND ONCOGENESIS INVIVO. *Cancer Research* 40:1493-1500.
- S7. Farinas, J., and A. S. Verkman. 1996. Cell volume and plasma membrane osmotic water permeability in epithelial cell layers measured by interferometry. *Biophys J* 71:3511-3522.
- S8. Hochmuth, R. M. 2000. Micropipette aspiration of living cells. *J Biomech* 33:15-22.

- S9. Fuller, T. F., and J. Newman. 1992. Experimental Determination of the Transport Number of Water in Nafion 117 Membrane. *Journal of The Electrochemical Society* 139:1332-1337.